MUNI SCI

Synchronization in Dynamical Systems from the Bifurcation Theory Point of View

Doctoral Thesis Defence

Jan Ševčík (sevcik@math.muni.cz)
Lenka Přibylová (supervisor), **Veronika Eclerová** (consultant)

Department of Mathematics and Statistics, Faculty of Science, Masaryk University

February 4, 2026

Outline

Focal epilepsy and VHFOs/UFOs

- **Synchronization** of large neuronal populations $\rightsquigarrow$ recurrent spontaneous seizures
- Modeling via a population of coupled neurons/neural masses
- **HFOs**: 80 – 600 Hz, **VHFOs**: 600 – 2 000 Hz, **UFOs**: above 2 000 Hz
- Possible (physiological) frequencies: at most $\sim$ 600 Hz

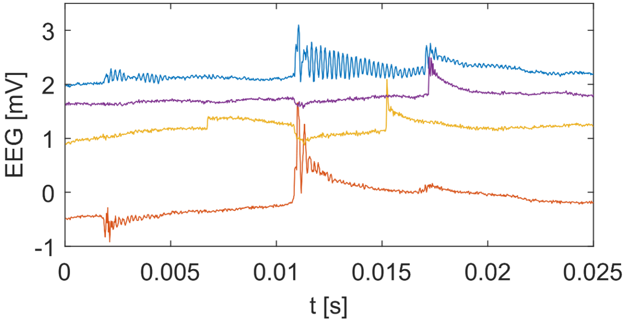

Figure: An example of real UFOs

Focal epilepsy and VHFOs/UFOs

- **Synchronization** of large neuronal populations $\rightsquigarrow$ recurrent spontaneous seizures
- Modeling via a population of coupled neurons/neural masses
- **HFOs**: 80 – 600 Hz, **VHFOs**: 600 – 2 000 Hz, **UFOs**: above 2 000 Hz
- Possible (physiological) frequencies: at most $\sim$ 600 Hz

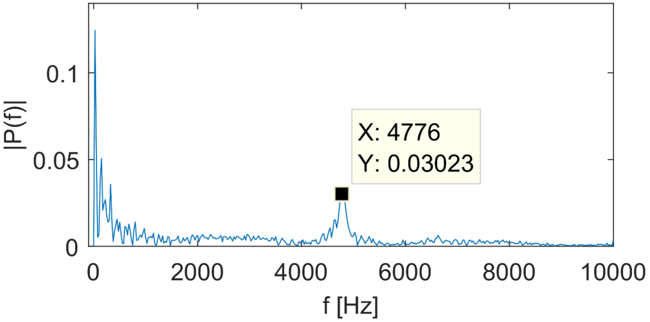

Figure: A periodogram of the signal with real UFOs

VHFOs — questions and objectives

Overall (medical) objective

- HFOs — biomarker, maybe physiological,
  VHFOs/UFOs — new biomarker, non-physiological
- Possible explanation of VHFOs/UFOs emergence leading to a deeper understanding of electrical events in the human brain

Mathematical objectives

- Can we simulate such VHFOs/UFOs using models of neuronal networks?
- Which phenomenon is behind the emergence of VHFOs/UFOs?

VHFOs — questions and objectives

Overall (medical) objective

- HFOs — biomarker, maybe physiological,
  VHFOs/UFOs — new biomarker, non-physiological
- Possible explanation of VHFOs/UFOs emergence leading to a deeper understanding of electrical events in the human brain

Mathematical objectives

- Can we simulate such VHFOs/UFOs using models of neuronal networks?
- Which phenomenon is behind the emergence of VHFOs/UFOs?

VHFOs — questions and objectives

Overall (medical) objective

- HFOs — biomarker, maybe physiological,
  VHFOs/UFOs — new biomarker, non-physiological
- Possible explanation of VHFOs/UFOs emergence leading to a deeper understanding of electrical events in the human brain

Mathematical objectives

- Can we simulate such VHFOs/UFOs using models of neuronal networks?
- Which phenomenon is behind the emergence of VHFOs/UFOs?

VHFOs — questions and objectives

Overall (medical) objective

- HFOs — biomarker, maybe physiological,
  VHFOs/UFOs — new biomarker, non-physiological
- Possible explanation of VHFOs/UFOs emergence leading to a deeper understanding of electrical events in the human brain

Mathematical objectives

- Can we simulate such VHFOs/UFOs using models of neuronal networks?
- Which phenomenon is behind the emergence of VHFOs/UFOs?

Interneuron model (IN)

- Model equations:[1]

$$\begin{cases} C\dfrac{d}{dt}V = I_{ext} - \overbrace{\bar{g}_L(V - V_L)}^{I_L} - \overbrace{\bar{g}_{Na} m_\infty^3(V) h (V - V_{Na})}^{I_{Na}} - \overbrace{\bar{g}_K n^4 (V - V_K)}^{I_K} \\ \dfrac{d}{dt}h = \dfrac{h_\infty(V) - h}{\tau_h(V)} \qquad \dfrac{d}{dt}n = \dfrac{n_\infty(V) - n}{\tau_n(V)} \end{cases}$$

- Steady-state functions and time functions:
  - Na^{2+}-channel:

$$m_\infty(V) = (1 + \exp[-0.08(V + 26)])^{-1}$$
$$h_\infty(V) = (1 + \exp[0.13(V + 38)])^{-1}$$
$$\tau_h(V) = 0.6(1 + \exp[-0.12(V + 67)])^{-1}$$

  - K^{+}-channel:

$$n_\infty(V) = (1 + \exp[-0.045(V + 10)])^{-1}$$
$$\tau_n(V) = 0.5 + 2(1 + \exp[0.045(V - 50)])^{-1}$$

[1] White, J. et al. (1998). Synchronization and oscillatory dynamics in heterogeneous, mutually inhibited neurons.

Interneuron model (IN)

- Model equations:[1]

$$
\begin{cases}
C\dfrac{d}{dt}V = I_{ext} - \overbrace{\bar{g}_L(V - V_L)}^{I_L} - \overbrace{\bar{g}_{Na}m_\infty^3(V)h(V - V_{Na})}^{I_{Na}} - \overbrace{\bar{g}_K n^4(V - V_K)}^{I_K} \\
\dfrac{d}{dt}h = \dfrac{h_\infty(V) - h}{\tau_h(V)} \qquad \dfrac{d}{dt}n = \dfrac{n_\infty(V) - n}{\tau_n(V)}
\end{cases}
$$

- Typical parameter values for a hippocampal interneuron:
  - Capacitance: $C = 1$ [μF/cm^2]
  - Externally applied current: $I_{ext} \in [-2, 27]$ [μA/cm^2]
  - Maximum conductances: $\bar{g}_L = 0.1$, $\bar{g}_{Na} = 30$, $\bar{g}_K = 20$ [mS/cm^2]
  - Equilibrium potentials: $V_L = -60$, $V_{Na} = 45$, $V_K = -80$ [mV]
- Crucial role in the synchronization of hippocampal neuronal activity

[1] White, J. et al. (1998). Synchronization and oscillatory dynamics in heterogeneous, mutually inhibited neurons.

Types of dynamics

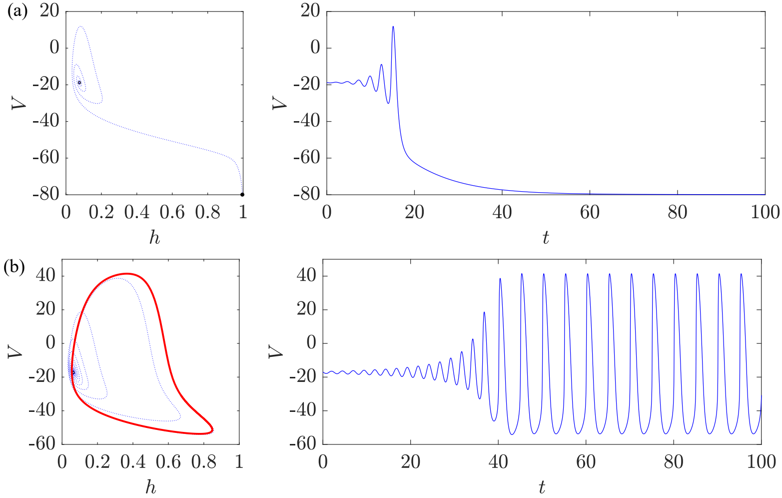

Figure: Orbits tending to (a) a stable equilibrium (resting state) for $I_{ext} = -2$ and (b) a limit cycle (spiking dynamics) for $I_{ext} = 8$

Model dynamics w.r.t. I_{ext}

- Variation of I_{ext} can switch the model dynamics
- **Rest./overstim. state** (EPs), **spiking dynamics** (min & max of LCs)
- — stable, - - unstable

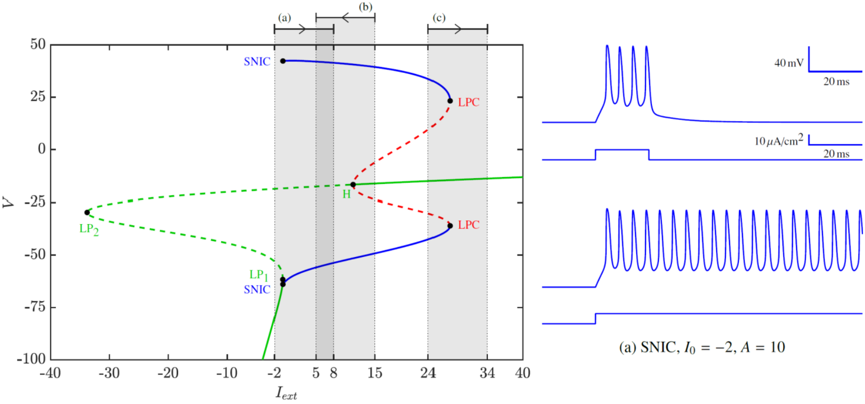

Figure: A bifurcation diagram of V w.r.t. I_{ext}, along with the stimuli ranges

Neuronal network of N coupled interneurons

- Symmetrical gap-junctional coupling ε_{ij}:

$$\begin{cases} C_i \frac{d}{dt} V_i = I_{ext} - \bar{g}_L (V_i - V_L) - \bar{g}_{Na} m_\infty^3 (V_i) h_i (V_i - V_{Na}) \\ \qquad\qquad\qquad\qquad - \bar{g}_K n_i^4 (V_i - V_K) - \sum_{j=1}^{N} \varepsilon_{ij} (V_i - V_j) \\ \frac{d}{dt} h_i = \frac{h_\infty(V_i) - h_i}{\tau_h(V_i)} \qquad \frac{d}{dt} n_i = \frac{n_\infty(V_i) - n_i}{\tau_n(V_i)} \qquad i \in \{1, \dots, N\} \end{cases}$$

- Electrical synapses (gap junctions) $\rightsquigarrow$ **rapid** communication
- Chemical synapses $\rightsquigarrow$ delayed (**slow**) communication
- Equal parameters, different capacitances C_i

Two coupled INs

- Symmetrical gap-junctional coupling: $\varepsilon_{1,2} = \varepsilon_{2,1} = \varepsilon$

$$\begin{cases} C_1 \dfrac{d}{dt} V_1 = I_{ext} - \bar{g}_L (V_1 - V_L) - \bar{g}_{Na} m_\infty^3 (V_1) h_1 (V_1 - V_{Na}) \\ \qquad\qquad - \bar{g}_K n_1^4 (V_1 - V_K) - \varepsilon (V_1 - V_2) \\ \dfrac{d}{dt} h_1 = \dfrac{h_\infty(V_1) - h_1}{\tau_h(V_1)} \qquad \dfrac{d}{dt} n_1 = \dfrac{n_\infty(V_1) - n_1}{\tau_n(V_1)} \end{cases}$$

$$\begin{cases} C_2 \dfrac{d}{dt} V_2 = I_{ext} - \bar{g}_L (V_2 - V_L) - \bar{g}_{Na} m_\infty^3 (V_2) h_2 (V_2 - V_{Na}) \\ \qquad\qquad - \bar{g}_K n_2^4 (V_2 - V_K) - \varepsilon (V_2 - V_1) \\ \dfrac{d}{dt} h_2 = \dfrac{h_\infty(V_2) - h_2}{\tau_h(V_2)} \qquad \dfrac{d}{dt} n_2 = \dfrac{n_\infty(V_2) - n_2}{\tau_n(V_2)} \end{cases}$$

- Equal parameters, different capacitances C_1, C_2

Types of dynamics (w.r.t. C_1 and ε)

- In-phase synchrony (IPS)
- Quasiperiodic behavior (QB)
- Anti-phase synchrony (APS)
- Quasiperiodic anti-phase synchrony (QAPS)
- Resting (RS) or overstimulated state (OS)
- Subthreshold oscillation (STO)

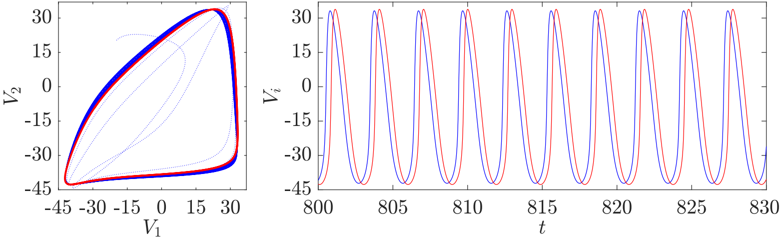

Figure: An orbit tending to the IPS for $C_1 = 0.99$, $\varepsilon = 0.04$

Types of dynamics (w.r.t. C_1 and ε)

- In-phase synchrony (IPS)
- Quasiperiodic behavior (QB)
- Anti-phase synchrony (APS)
- Quasiperiodic anti-phase synchrony (QAPS)
- Resting (RS) or overstimulated state (OS)
- Subthreshold oscillation (STO)

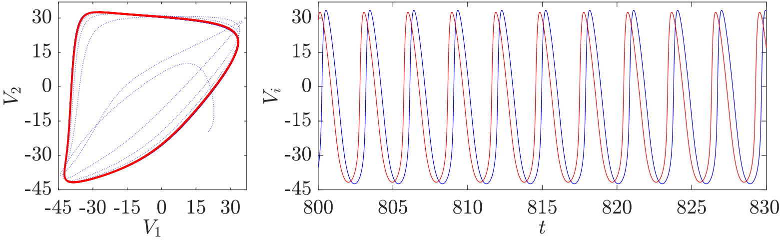

Figure: An orbit tending to the IPS for $C_1 = 1.01$, $\varepsilon = 0.04$

Types of dynamics (w.r.t. C_1 and ε)

- In-phase synchrony (IPS)
- Quasiperiodic behavior (QB)
- Anti-phase synchrony (APS)
- Quasiperiodic anti-phase synchrony (QAPS)
- Resting (RS) or overstimulated state (OS)
- Subthreshold oscillation (STO)

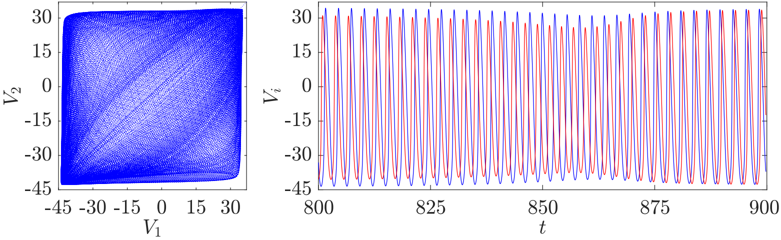

Figure: A quasiperiodic orbit for $C_1 = 0.95$, $\varepsilon = 0.04$

Types of dynamics (w.r.t. C_1 and ε)

- In-phase synchrony (IPS)
- Quasiperiodic behavior (QB)
- Anti-phase synchrony (APS)
- Quasiperiodic anti-phase synchrony (QAPS)
- Resting (RS) or overstimulated state (OS)
- Subthreshold oscillation (STO)

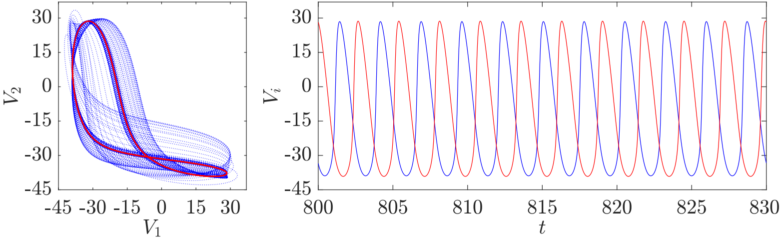

Figure: An orbit tending to the APS for $C_1 = 0.99$, $\varepsilon = 0.035$

Types of dynamics (w.r.t. C_1 and ε)

- In-phase synchrony (IPS)
- Quasiperiodic behavior (QB)
- Anti-phase synchrony (APS)
- Quasiperiodic anti-phase synchrony (QAPS)
- Resting (RS) or overstimulated state (OS)
- Subthreshold oscillation (STO)

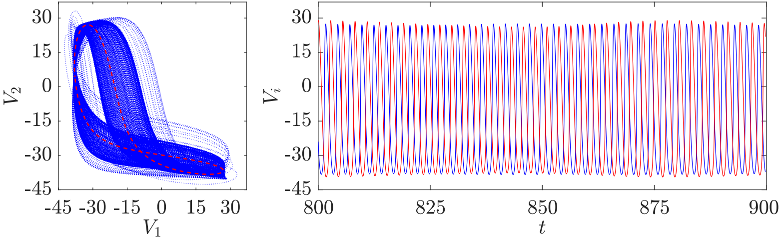

Figure: A quasiperiodic orbit on an invariant anti-phase torus (QAPS) near the unstable APS for $C_1 = 0.99$, $\varepsilon = 0.04$

Types of dynamics (w.r.t. C_1 and ε)

- In-phase synchrony (IPS)
- Quasiperiodic behavior (QB)
- Anti-phase synchrony (APS)
- Quasiperiodic anti-phase synchrony (QAPS)
- Resting (RS) or overstimulated state (OS)
- Subthreshold oscillation (STO)

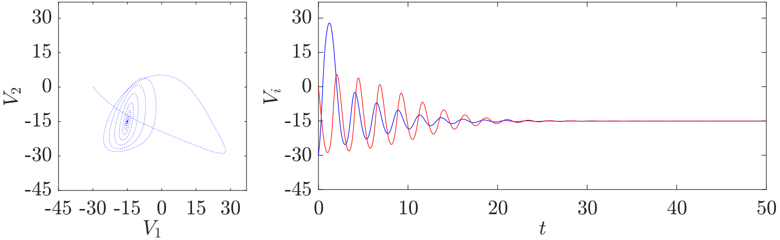

Figure: An orbit tending to the RS for $C_1 = 0.99$, $\varepsilon = 0.04$

Types of dynamics (w.r.t. C_1 and ε)

- In-phase synchrony (IPS)
- Quasiperiodic behavior (QB)
- Anti-phase synchrony (APS)
- Quasiperiodic anti-phase synchrony (QAPS)
- Resting (RS) or overstimulated state (OS)
- Subthreshold oscillation (STO)

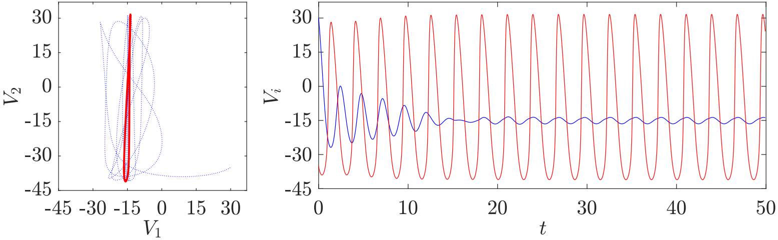

Figure: An orbit tending to a limit cycle representing the STO of the first neuron for $C_1 = 0.99$, $\varepsilon = 0.04$

Types of dynamics (w.r.t. C_1 and ε)

- In-phase synchrony (IPS)
- Quasiperiodic behavior (QB)
- Anti-phase synchrony (APS)
- Quasiperiodic anti-phase synchrony (QAPS)
- Resting (RS) or overstimulated state (OS)
- Subthreshold oscillation (STO)

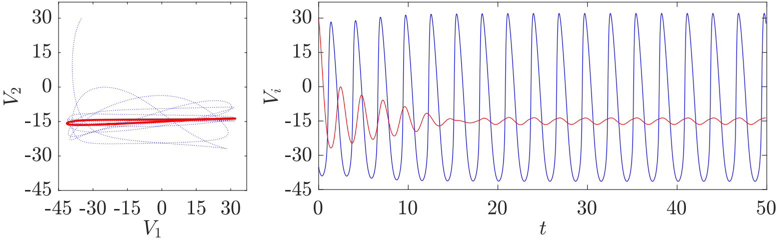

Figure: An orbit tending to a limit cycle representing the STO of the second neuron for $C_1 = 0.99$, $\varepsilon = 0.04$

Frequency of the IPSs and APS w.r.t. C_1

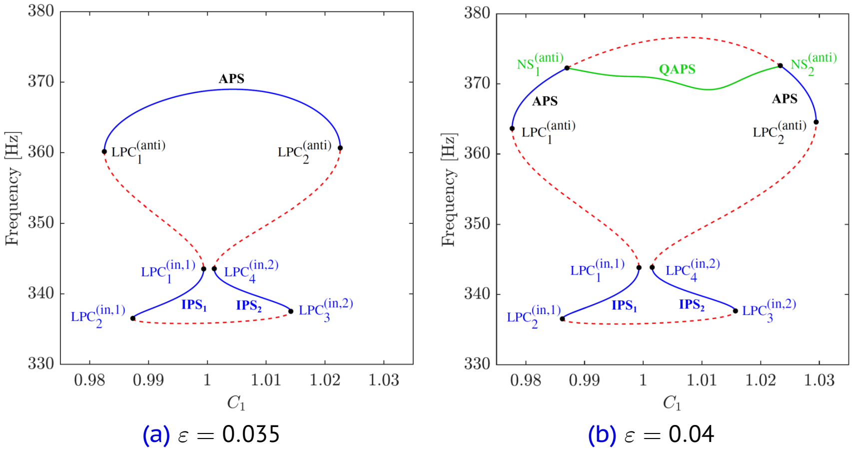

Figure: Frequency of the IPSs, APS (and QAPS) w.r.t. C_1, while $C_2 = 1$ is fixed

- Presence of **bistability** for a relatively wide range of C_1

Arnold tongues in (C_1, C_2) and (C_1, ε)-planes

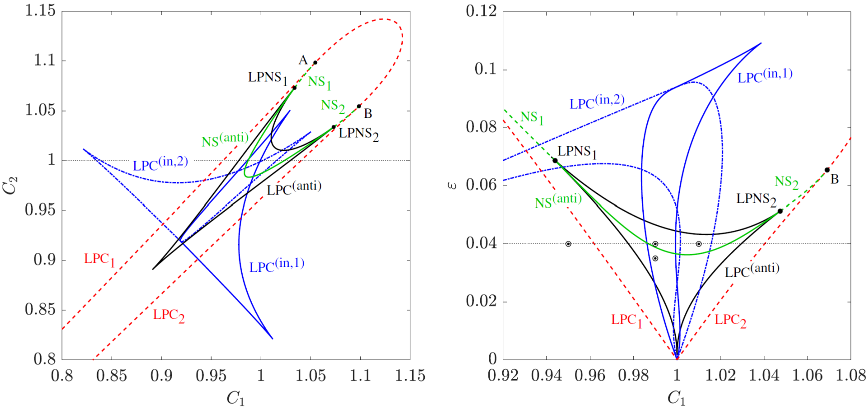

(a) $\varepsilon = 0.04$ (b) $C_2 = 1$

- **Blue**/**black** lines – LPC for two symmetrical **IPSs** and one **APS**
- **Red** dashed line – LPC for two unstable periodic solutions
- **Green** line – NS bifurcation of the APS

Modeling EEG signal

- Real EEG signals (LFP) − local electrical events
- Combined signal: $V = \sum_{i=1}^{N} V_i$

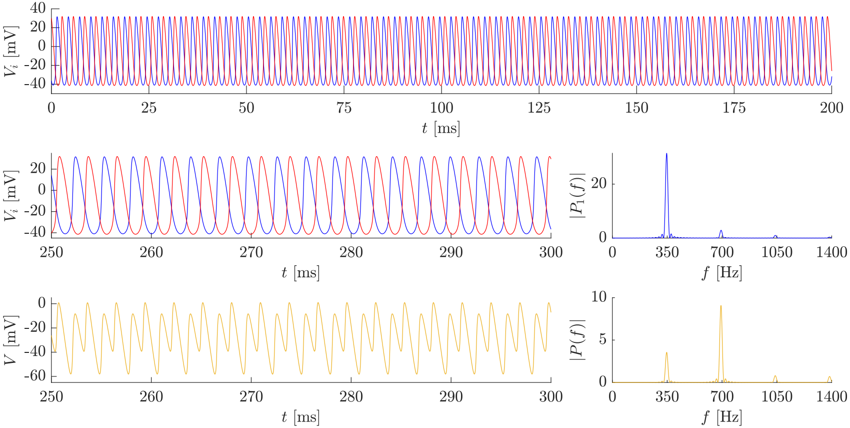

Doubled dominant frequency in $V = V_1 + V_2$

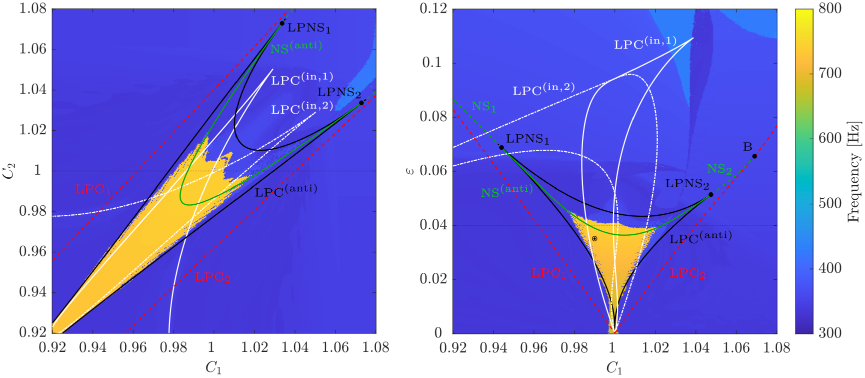

(a) $\varepsilon = 0.04$ (b) $C_2 = 1$

- White/**black** lines – LPC for two symmetrical IPSs and one **APS**
- Red dashed line – LPC for two unstable periodic solutions
- Green line – NS bifurcation of the APS

Doubled dominant frequency in $V = V_1 + V_2$

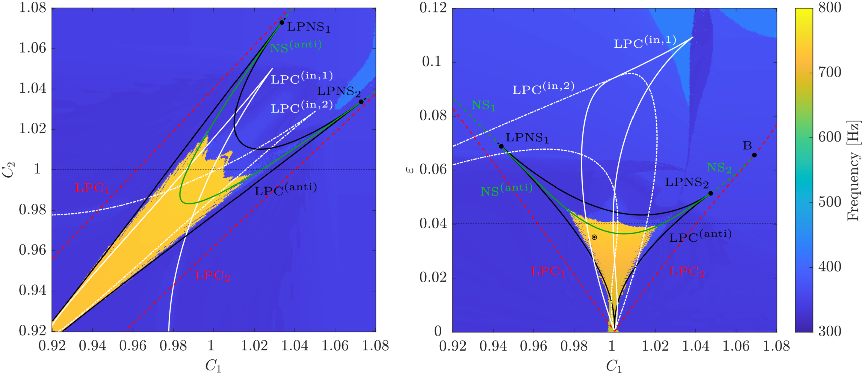

(a) $\varepsilon = 0.04$ (b) $C_2 = 1$

- Background color – the **dominant** frequency in the summed signal $V = V_1 + V_2$
- ICs – near the APS (if applicable)

Model dynamics w.r.t. I_{ext}

- $C_1 = 0.99$, $C_2 = 1$, $\varepsilon = 0.04$
- Significantly more complex dynamics compared to a single cell
- Relatively similar overall bifurcation structure

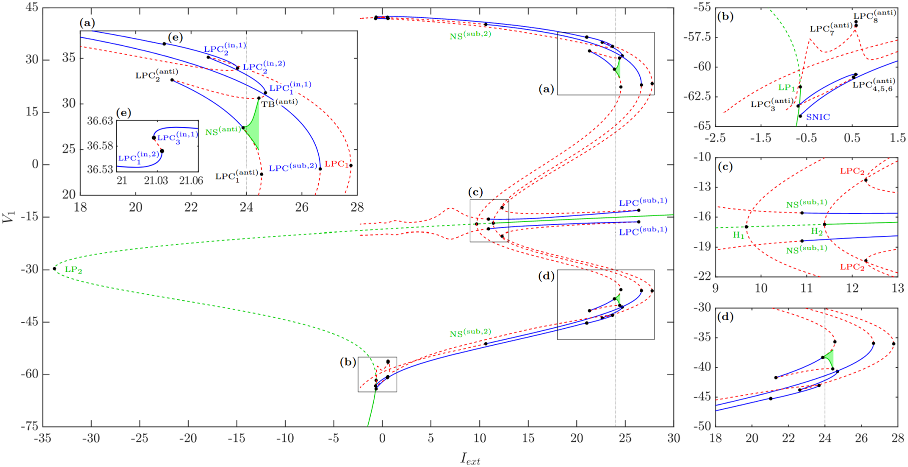

Variation of I_{ext} can switch the dynamics: RS ⇝ IPS

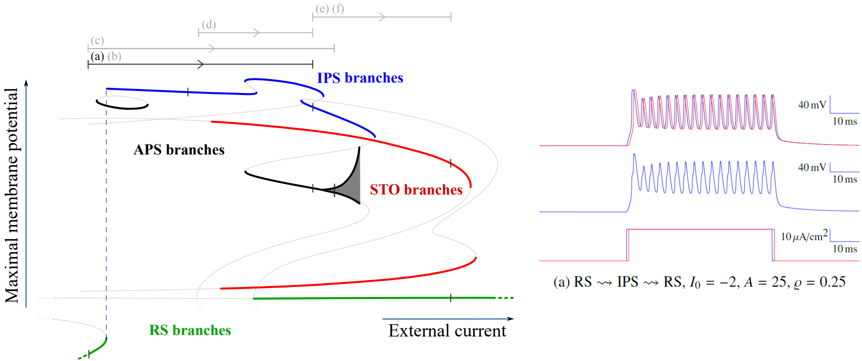

Figure: A simplified scheme of the bifurcation diagram w.r.t. I_{ext}, along with the stimuli ranges

- I_0 – baseline current
- A – amplitude
- ϱ – relative propagation delay for the second neuron

Variation of I_{ext} can switch the dynamics: RS $\leftrightsquigarrow$ APS

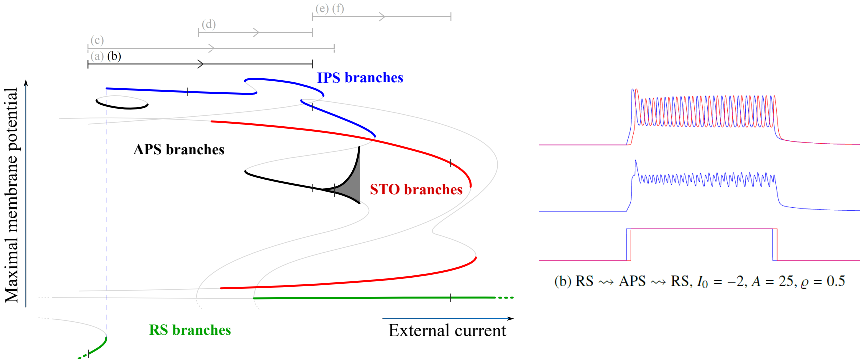

Figure: A simplified scheme of the bifurcation diagram w.r.t. I_{ext}, along with the stimuli ranges

- I_0 − baseline current
- A − amplitude
- ϱ − relative propagation delay for the second neuron

80 coupled INs — simulation setting (1)

- $N = 80$ INs, $\mathcal{P}_1 = \{1, \ldots, 40\}$, $\mathcal{P}_2 = \{41, \ldots, 80\}$
- $C_i \sim TN(1, 0.03^2, 0.91, 1.09), \; i \in \mathcal{P}_1 \cup \mathcal{P}_2$
- Symmetrical gap-junctional coupling

$$\varepsilon_{ij} = \begin{cases} 0, & i = j, \\ 0.01, & (i,j) \in \mathcal{P}_1 \times \mathcal{P}_1 \cup \mathcal{P}_2 \times \mathcal{P}_2, \quad i \neq j, \\ 0.001, & \text{otherwise} \end{cases}$$

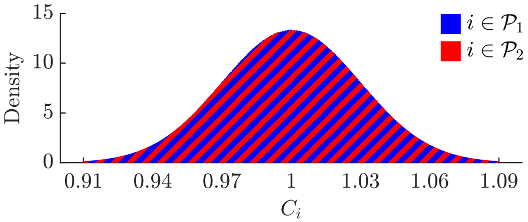

Figure: Capacitances

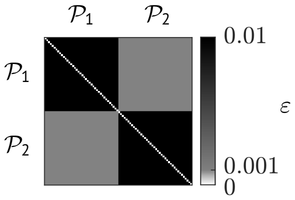

Figure: Coupling

80 coupled INs – simulation setting (2)

- Equal ICs near the collective resting state for $I_{ext} = -2$
- Random input

$$I_{ext,i}(t) = \underbrace{-2 + p_i(t)}_{deter.} + \underbrace{\xi_i(t)}_{stoch.}, \quad \xi_i(t) \overset{ind}{\sim} N(0, 1^2), \quad i \in \mathcal{P}_1 \cup \mathcal{P}_2$$

with time-distributed stimuli given by

$$\varrho_i \sim TN(0, 0.2^2, -0.6, 0.6), \quad i \in \mathcal{P}_1,$$
$$\varrho_i \sim TN(r, 0.2^2, r - 0.6, r + 0.6), \quad i \in \mathcal{P}_2$$

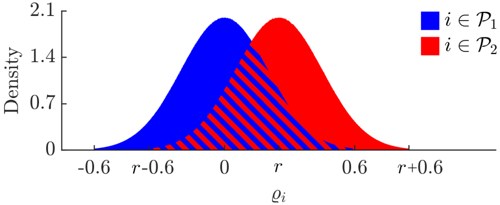

Figure: Relative delay

Collective in-phase behavior for $r = 0.25$

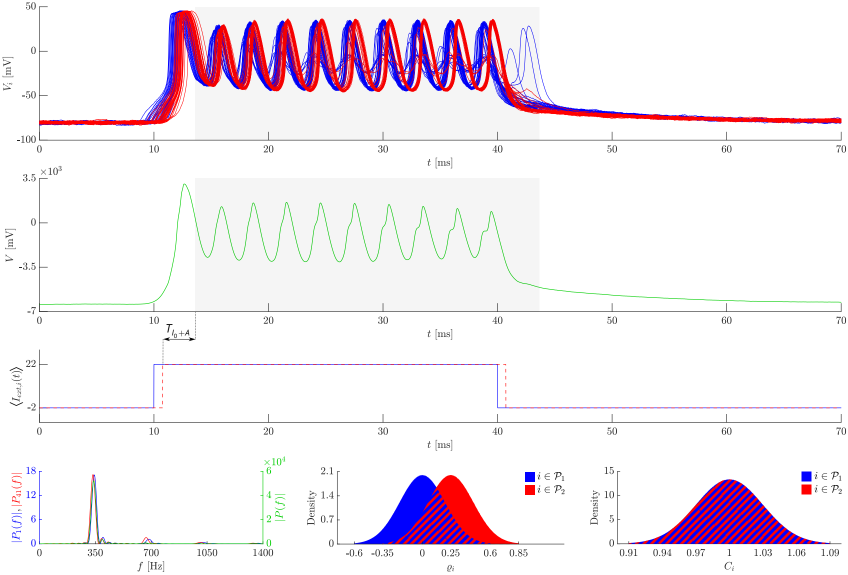

Collective anti-phase behavior for $r = 0.5$

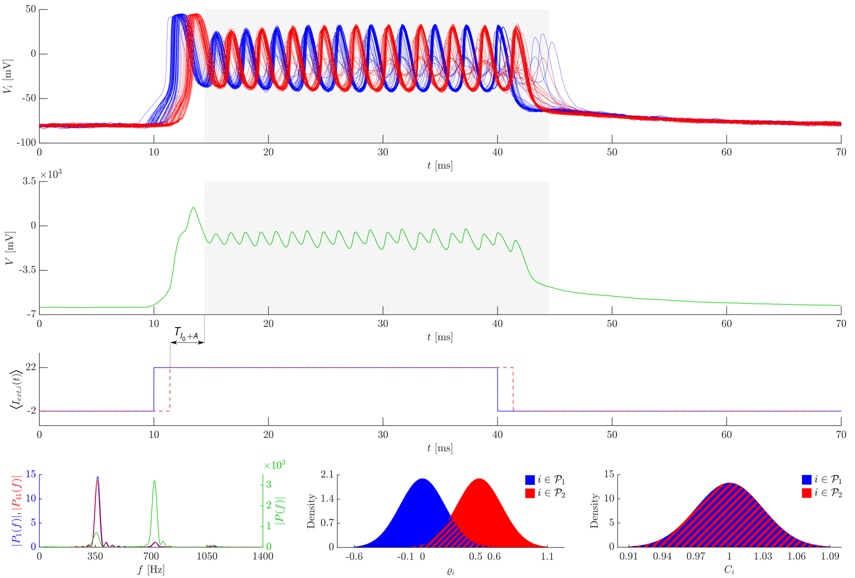

Comparison of small- and large-scale networks

- Evoked neuronal response within 30 ms after the stimulus onset

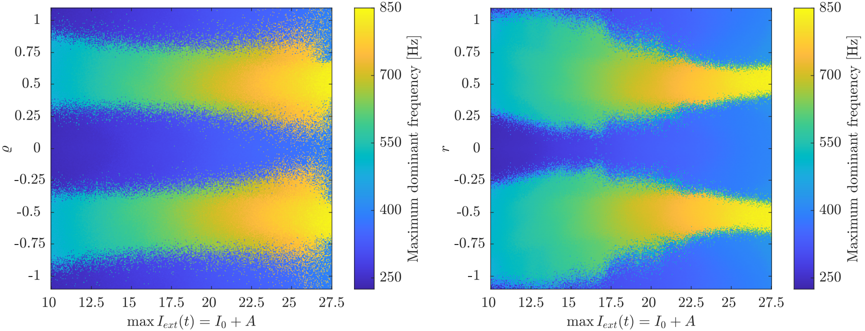

(a) 2 coupled INs (b) 2 × 40 coupled INs

Figure: The **maximum dominant frequency** in the summed signal *V*

Comparison of small- and large-scale networks

- Evoked neuronal response within 30 ms after the stimulus onset
- Increasing the network size **enhances** the probability of achieving APB

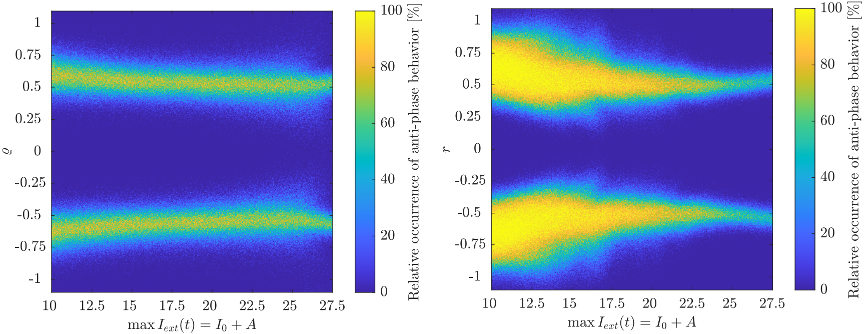

(a) 2 coupled INs

(b) 2 × 40 coupled INs

Figure: The **relative occurrence** of the generated APB

VHFOs — possible mathematical explanation

Mathematical objectives

- Can we simulate such VHFOs/UFOs using models of neuronal networks?
- Which phenomenon is behind the emergence of VHFOs/UFOs?

Possible answers

- **Weakened connections** between similar neuronal populations (near-identical neurons) can result in apparent VHFOs
- **Anti-phase** (phase-shift) **synchronization** of neuronal subpopulations (neuronal firing)

VHFOs — possible mathematical explanation

Mathematical objectives

- Can we simulate such VHFOs/UFOs using models of neuronal networks?
- Which phenomenon is behind the emergence of VHFOs/UFOs?

Possible answers

- **Weakened connections** between similar neuronal populations (near-identical neurons) can result in apparent VHFOs
- **Anti-phase** (phase-shift) **synchronization** of neuronal subpopulations (neuronal firing)

VHFOs — possible mathematical explanation

Mathematical objectives

- Can we simulate such VHFOs/UFOs using models of neuronal networks?
- Which phenomenon is behind the emergence of VHFOs/UFOs?

Possible answers

- **Weakened connections** between similar neuronal populations (near-identical neurons) can result in apparent VHFOs
- **Anti-phase** (phase-shift) **synchronization** of neuronal subpopulations (neuronal firing)

Thank You for Your Attention!

References

Ševčík, J., & Přibylová, L. (2025). Cycle multistability and synchronization mechanisms in coupled interneurons: In-phase and anti-phase dynamics under current stimuli. *Applied Mathematics and Computation*, *503*, 129500. doi: 10.1016/j.amc.2025.129500.

Přibylová, L., **Ševčík, J.**, Eclerová, V., Klimeš, P., Brázdil, M., & Meijer, H. G. (2024). Weak coupling of neurons enables very high-frequency and ultra-fast oscillations through the interplay of synchronized phase shifts. *Network Neuroscience*, *8* (1), 293–318. doi: 10.1162/netn_a_00351.

Záthurecký, J., Eclerová, V., **Ševčík, J.**, Zapadlo, Š., & Přibylová, L. (2025). Phase shifts inside Arnold tongues of weakly coupled oscillators. *Communications in Nonlinear Science and Numerical Simulation*, *145*, 108729. doi: 10.1016/j.cnsns.2025.108729.

Přibylová, L., **Ševčík, J.**, Halmazňa, T., Husa, Š., Kajanová, L., Malárik, P., Polách, M., Zapadlo, Š., & Eclerová, V. (2025). Chaos links dendritic calcium to bursting in hippocampal pyramidal cells. *Chaos, Solitons & Fractals*, *197*, 116517. doi: 10.1016/j.chaos.2025.116517.

(1) Monography $\times$ a commented collection of papers

- **Coherent restructuring** and **unification** of all results into a single, logically consistent narrative
- **Space to integrate additional results** that could not be included in journal articles
- Harmonized **heterogeneous publications** with different scopes, journals, and levels of my authorship contribution
- Eliminated **redundancy** and **overlap** in motivation, methodology, and model descriptions across papers
- **Conceptual** (not chronological) **organization of results**
- Unified findings within a **bifurcation-theoretic view of synchronization** (official thesis assignment), improving clarity and accessibility

(2) Author's contributions

- Published papers = **joint results** of the entire research team $\rightsquigarrow$ a strict separation of individual contributions non-trivial (see Section List of Published Works)
- I collaborated on **all results** included in the dissertation
- All results not previously published in journal articles are **entirely my own**
- My core contributions:
  - **numerical computations** and **simulations**,
  - **visualization** and **graphical presentation** of results,
  - **software (co-)development** (including complete code implementation or tuning/refactoring),
  - **writing** and **structuring** of the thesis text

(3) Broader context and relevance to epilepsy research

- Deeper understanding of **electrical events in the human brain**, possible **mechanisms underlying the onset of epilepsy seizures**
- **Potentials of UFOs**
  - More accurate **detection and localization** of epileptogenic zones (improved **surgical outcomes**)
- **Contribution of bifurcation diagrams**
  - **Systematic map** of dynamical regimes (DRs)
  - **Robustness** of DRs under small parameter perturbations
  - Reveal **transitions between DRs** as model parameters vary
  - Diagrams w.r.t. I_{ext} show **response** to:
    - fluctuating synaptic input,
    - information transfer from the surrounding network,
    - externally induced modulation (e.g., stimulation or pharmacological effects)
- Principled framework for **interpreting and predicting transitions** to epileptic activity

(4) Morris–Lecar (ML) × Interneuron (IN) model

- **Model type and biological interpretation**
  - Both are **conductance-based neuronal models**
  - ML: a **pyramidal cell**, IN: an **interneuron**
- **Single-cell dynamics**
  - Both are **class-I excitable models**
  - Similar bifurcation structure and **comparable dynamical repertoire** (resting state, spiking, overstimulated state)
  - Physiological firing ranges (ML: $\sim$ **0–60 Hz**, IN: $\sim$ **0–400 Hz**)
- **Network-level bifurcation structure**
  - The bifurcation structure of the **two-cell interneuronal system** is **significantly richer** than that of two ML neurons
  - APS in the ML system is **more robust** (longer hyperpolarization)
- **Role within the thesis**
  - Analysis started with the **ML**, further extended to the **IN**
  - **Non-model-specific nature** of the APS

(5) Declaration on the use of AI tools

Dissertation, page *iv*

"Throughout the preparation of this dissertation, I used ChatGPT (OpenAI, 2024) as a supplementary writing and editing tool. It assisted in refining the clarity of formulations, improving stylistic consistency, and resolving various technical matters related to terminology and LaTeX. ***The tool was employed exclusively to support the presentation of ideas; it did not contribute to any of the scientific results, analyses, or conclusions presented herein****."*

- Used primarily for individual sentences rather than entire paragraphs

(A.1) Solver tolerances and scale separation (ode45)

- Neuronal model exhibit **separated scales**:
  - membrane potential (V): $\mathcal{O}(10)$,
  - gating variables: $\mathcal{O}(10^{-1})$
- `RelTol` controls the **relative accuracy** of large-amplitude variables
  - `RelTol` $= 10^{-3}$ allows $\mathcal{O}(10^{-2})$ accuracy for V,
  - sufficient for capturing frequencies, phases, and bifurcation structure
- `AbsTol` protects **small-amplitude variables**
  - `AbsTol` $= 10^{-6}$ prevents numerical suppression of gating dynamics,
  - ensures stability near equilibria and bifurcation boundaries
- **Large** `RelTol` & **small** `AbsTol` is thus **computationally efficient** (especially in grid simulations of systems with separated scales)
- **Adaptive time step** with **upper bound** `MaxStep` given by `dt` (IN)
  - Fixed choice `dt` $= 0.01$ (based on observed system dynamics)

(A.2) Stiffness and numerical issues

- **Time-domain simulations**
  - typically strongly separated time scales,
  - explicit solvers (e.g. `ode45`) require **very small time steps**
  - No stiffness-related issues for **IN2**
  - Stiffness encountered for **ML2** and **vdP2**
- **Parameter continuation** (`MatCont`)
  - Near ill-conditioned points during continuation
  - Numerical difficulties near **bifurcation points** or **sharp transitions**
  - Typically suppressed by:
    - adaptive step size control,
    - adjustment of tolerances (`RelTol`, `AbsTol`),
    - refined discretization of limit cycles

(B.1 & B.2) Discontinuities: time-domain and continuation

- **Time-domain simulations**
  - ode45 assumes a **smooth RHS** $\rightsquigarrow$ loss of accuracy or solver failure
    - Possible solution: **event handling** & **piecewise integration**
  - **Euler–Maruyama scheme**:
    - natural inclusion of **noise** (stochastic simulations),
    - ability to handle **discontinuous forcing** (shocks, jumps),
    - lower order of accuracy,
    - requirement of sufficiently small time step dt
- **Parameter continuation** (MatCont)
  - Relies on derivatives and **Jacobian matrices**
  - Requires a **smooth** (at least C^1) vector field
    - Discontinuities or switching mechanisms not admissible
    - Switches commonly handled by **regularization** (e.g. smooth sigmoid-type approximations)

(B.3) Lyapunov definition of chaos

- **Sensitivity to initial conditions**
- Quantified by a **positive maximal Lyapunov exponent** (MLE)

$$\lambda_{\text{max}} > 0$$

- Nearby trajectories diverge **exponentially in time**

$$\|\delta \boldsymbol{x}(t)\| \approx \mathrm{e}^{\lambda_{\text{max}} t} \|\delta \boldsymbol{x}(0)\|$$

- Known as the **butterfly effect**:
  - arbitrarily small perturbations $\rightsquigarrow$ large long-term differences,
  - limits long-term predictability of the system
- Standard, **operational definition** in numerical studies

MASARYK UNIVERSITY